A Three-Degree-of-Freedom Anthropomorphic Oculomotor Simulator

Young-Bong Bang, Jamie K. Paik*, Bu-Hyun Shin, and Choongkil Lee

Abstract: For a sophisticated humanoid that explores and learns its environment and interacts with humans, anthropomorphic physical behavior is much desired. The human vision system orients each eye with three-degree-of-freedom (3-DOF) in the directions of horizontal, vertical and torsional axes. Thus, in order to accurately replicate human vision system, it is imperative to have a simulator with 3-DOF end-effector. We present a 3-DOF anthropomorphic oculomotor system that reproduces realistic human eye movements for human-sized humanoid applications. The parallel link architecture of the oculomotor system is sized and designed to match the performance capabilities of the human vision. In this paper, a biologically-inspired mechanical design and the structural kinematics of the prototype are described in detail. The motility of the prototype in each axis of rotation was replicated through computer simulation, while performance tests comparable to human eye movements were recorded.

Keywords: Eye simulator, humanoid, oculomotor, parallel mechanism, robot vision, three-degree-of-freedom manipulator, vision system.

1. INTRODUCTION

The advances in robots and humanoids in recent years have fascinated many people who have regarded robots simply as fast and strong limbs to execute industrial heavy-duty tasks. Nowadays, sophisticated humanoids are able to interact with their environment, including humans, to study and gain understanding of the world that surrounds them. Humanoids similar to humans in their behavioral algorithms and physique, can not only replicate human-like actions, but also help medical professionals, scientists and engineers to deepen the understanding of human conduct in various situations and environments [1].

Designing and developing a humanoid with anthropomorphic physique and capabilities introduces many obstacles because the human body is extremely complex and yet relatively robust in mechanical respects, let alone the intelligence. Therefore, even with current advances in research, robots may reproduce, but yet to completely duplicate the human's body movements or performance in exact shape and form. The reason for this is because engineers face the immediate problem of acquiring actuators or designing structures that are compact in size but still be able to provide sufficient torque and power. Therefore, contemporary humanoids and animaloids tend to eliminate a degree-of-freedom or reduce mechanical capabilities.

The same type of problem arises with reproducing the human vision system. The human eyeball, upon stereotyped neural commands, achieves precise and rapid positioning (saccadic movements), and stable tracking and fixation (smooth pursuit) [2]. The orientations of each eye are controlled by three sets of extraocular muscles that stretch and contract to provide tensions in 3-DOF. To develop a simulator that mimics the capabilities of the human vision system in 3-DOF in a plausible size is a challenging engineering task. Therefore, in designing anatomically unconscious humanoids, it has been a popular choice to limit the degree of freedom in the robot vision to 2-DOF by eliminating the torsion axis.

To attain human-like eye motions, an eye simulator should maintain a constant center of rotation that is placed at a similar position as humans, and produces smooth rotations regardless of the speed, acceleration and path of the movement. Without a full degree-of-freedom, a compact volume, or a specific mechanical performance, the reproduced eye movement would be

Manuscript received April 6, 2005; revised September 27, 2005; accepted December 19, 2005. Recommended by Editorial Board member Hyoukryeol Choi under the direction of Editor Jae-Bok Song. This work was supported by the Neuroinformatics Research Program of the Korea Ministry of Science and Technology.

Young-Bong Bang, Jamie K. Paik, and Bu-Hyun Shin are with the School of Mechanical and Aerospace Engineering, Seoul National University, San 56-1, Sillim-dong, Gwanak-gu, Seoul 151-742, Korea (e-mails: {ybbang, jamie79, sbh4462} @snu.ac.kr).

Choongkil Lee is with the Department of Psychology, Seoul National University, San 56-1, Sillim-dong, Gwanak-gu, Seoul 151-742, Korea (e-mail: cklee@snu.ac.kr).

* Corresponding author.

discontinuous, spasmodic, or simply seem “robotic” and awkward. This means that a device may move but will not be able to give the feel of real human eyes. In the case of a single or 2-DOF eyeball simulator, images may be captured without the third axis of rotation, but reproducing human eye movement does require this third axis of rotation. Accurate and lively actions are main concern when future endeavors are placed toward more sophisticated interactive humanoids with vision system on a freely-moving head and body.

Two axes of camera frame could provide images that can be digitalized and vision processed to compensate for distortions. However, the torsion axis is crucial for realizing accurate human eye captured images with a proper sampling rate [3]. Besides, the software compensation process for a missing torsional rotation is computationally expensive and consequently disables simultaneous data acquisition. Only with the third torsion axis can the received images be realized in 3D properly [2].

Various types of humanoids are under development for achieving more lifelike and intelligent robots. A communication system which aims to transmit human emotions via humanoid EbR is introduced in [4]. EbR has 2-DOF movement in the eye for duplicating the original movements of the communicator. This 2-DOF in the robotic eyes is achieved with pulley wires, which are linked to DC motors. Hadaly-2 and WE-3 [5] are anthropomorphic robots that interact with human visitors using a vision system and a speech processing system. Hadaly-2 makes gestures and performs tasks using its anthropomorphic arms and head-eye system where WE-3 attempts to simulate human eye behavior including saccadic eyeball motions and pupil focusing angles with 2-DOF gimbals in the eye. Harvard binocular head [6] has two video cameras that jointly produce a total of 3-DOF rotations in two eyes: a symmetric pan/tilt motion and vergence motion (an anti-symmetric rotation about the vertical axis). Two AC servo-motors actuate the cameras that are placed in gimbals structure. The binocular robotic head [7] has a 3-DOF vision system which can reproduce torsional movement in the eye. Sociable robots that interact with humans such as Kismet [8] have humanlike features in order to create effective communication environment. Presently, Kismet has 2-DOF in its eyes without the eyelids and is able to track objects of interest or human cues. Because eyes have immediate and high communicative value [1], the anthropomorphic eye movements would be an effective feature of sociable humanoids that need to interact and communicate with humans. Gosselin and his colleagues developed the agile eye [9-10] which orients its camera mounted end effector in 3-DOF. It uses six sets of links (Fig. 1) that are actuated simultaneously for motion. The agile eye can also be adapted to robotic vision systems; however, the link mechanism surrounds the end effector and suggests some difficulty encasing the device behind a layer of a humanoid face.

In this paper, we present a 3-DOF anthropomorphic oculomotor simulator. This simulator utilizes a similar spherical link structure used in the agile eye [9] to recreate human eye characteristics with a life-sized humanoid application in mind. Unlike the agile eye, the anthropomorphic oculomotor simulator is built with bent link segments, whose design maintain motion path behind the eyeball. This unique link design enables the simulator to be installed in a life-sized humanoid head, while reproducing realistic high-speed human eye movements. In Section 2 of this paper, the oculomotor prototype is presented with mechanical details. Section 3 describes the inverse kinematics of the device for each rotational axis with respect to the coordinate of the eye movement. And the comparable working range of the developed oculomotor system to the human eye is given in Section 4. The actual performance of the prototype compared to the real human eye is given in Section 5.

2. MECHANICAL DESIGN

The anthropomorphic 3-DOF oculomotor system presented in this paper is, as its name suggests, an anatomically conscious simulator. Its mechanical design aims to mimic the mechanical behavior and capabilities of the human eye as closely as possible. One of the most distinct features of the human vision system is that it provides smooth and fast 3-DOF rotations in a very compact system. A human eyeball is actuated with six extra-ocular muscles: the medial and lateral recti, the superior and inferior recti, and the superior and inferior obliques [2]. Each set of muscles contributes to creating the rotations in three axes. These ocular muscles contract and stretch proficiently enabling saccadic and smooth motion in the eyeball. But to realize these characteristics in a robotic vision system, effective mechanical structure and actuators are necessary. The mechanism should be designed with a minimum moment of inertia in its moving parts in order to maintain the compact overall volume, because with a larger moment of inertia, the increase in actuator size is inevitable. Compact design for the structure is crucial, especially when two prototypes are to be put side by side for a human sized robot head.

The previously developed triple gimbals mechanism [11] attempts to minimize its overall size while keeping the degree of freedom in mind. In this paper, however, a link mechanism is presented in an effort to further decrease the size of the simulator using parallel link architecture. Also, by avoiding gimbal models, the moment of inertia of the structure

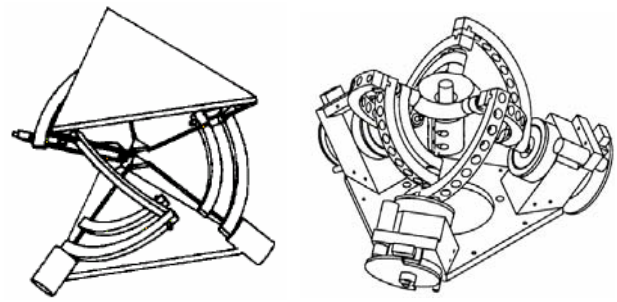

(a) General architecture spherical 3-DOF parallel-manipulator.
(b) CAD model of Agile Eye.

Fig. 1. Spherical 3-DOF parallel manipulator [9].

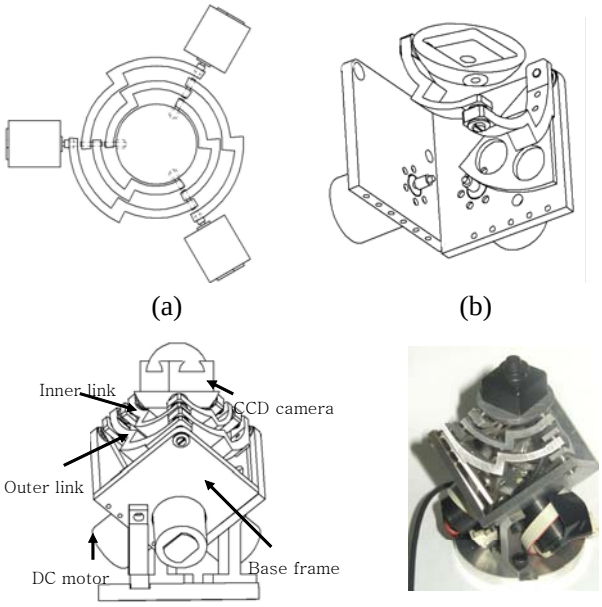

(a) (b) (c) (d)

(a) Expanded interlocked staged links.
(b) Link connection from the motor to the camera.
(c) CAD model of the prototype.
(d) Prototype.

Fig. 2. The 3-DOF anthropomorphic oculomotor simulator.

is minimized and so is its dynamic overshoot. The link architecture kinematics of the most recent model are quite similar to the agile eye (Fig. 1); however, the buckle design and its position and orientation around the center of rotation enables minimization of the range of protruding links and keeps the camera range under a spherical curve. Like the agile eye, the 3-DOF anthropomorphic ocular simulator [12] is composed of six spherical links that are adjoined to three actuators. The buckles in these six links allow them to make three sets of two-link (inner and outer links) stacks; the shape of the link enables the actuator installation to stay behind the base frame. The bird's eye-view on joint axes in Fig. 2(a) shows that the joints are collinear on three axes. The oculomotor simulator was designed to have the end-effector (camera) connected via two links from three actuators. These actuators move the gears to turn the outer links that lie on the same axis. And these outer links in turn move the inner links that are stacked right on top of the axis that is perpendicular to the outer link axis. Fig. 2(b) shows the link path from actuator to the end-effector of just one link set. Having the base frame fixate the actuators, the structure has minimum moving parts and minimized moment of inertia. Fig. 2(c) and 2(d) are the mechanical design of the simulator with all three sets of links.

The primary aim of the prototype development is to produce a simulator that bears mechanical resemblance to the human vision system in its size, behavior and performance of 800 deg/s and 30000 deg/s^2. The prototype of the 3-DOF anthropomorphic oculomotor simulator is designed to sufficiently achieve these values.

The prototype has a color CCD camera attached on the top, supported by a camera frame. This frame is linked to the spur and pinion gear via inner and outer links actuated by three DC servomotors Fig. 2(c). During the positioning and the controlling of the camera, all the links stay behind the face of the camera making a trace of a convex plane. For the prototype, a 27 mm diameter half-sphere eye cap is machined to cover the camera just up to the lens. Because an average human eye has a center of rotation at 13.5 mm behind the cornea, the center of rotation for the prototype is set accordingly.

In Fig. 3, the overall size of the prototype can be shown to be appropriate for a binocular robotic vision system. A woman's masquerade mask is placed on top of a prototype. Three outer and inner link sets are symmetric about the center of the rotation. This symmetry is desirable as it promotes an evenly

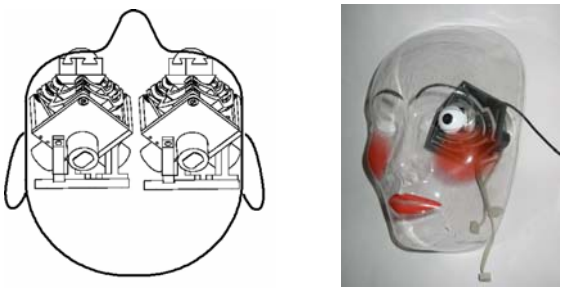

(a) (b)

(a) Visualization of two simulators inside a humanoid head.
(b) Prototype inside a masquerade mask.

Fig. 3. The prototype of the 3-DOF anthropomorphic oculomotor simulator.

distributed load on the motors. For the gimbals model, the actuator moving the outmost layer of the frame takes the most load when in motion. However, in the case of a spherical link type simulator, which has symmetrical and perpendicular link architecture, there is no one actuator that has a concentrated load. Because of this design, kinematics analysis becomes simpler and the structure is more stable than the gimbals model.

In building the simulator, no commercially available mini-motors can directly actuate the device with the desired torque output; it must be geared down. Here mini-DC servomotors (2224SR Faulhaber) with 8200 rpm (with no load) paired with encoder is chosen; together they measure Ø22mm x 25 mm. Since the motor's rated rpm is too high to produce the required torque, gearing down the high rpm is inevitable. Therefore, instead of using a commercially available multistage reduction gearbox (introduces a large backlash), a single gear (PDC = 78 mm) with a small module (m = 0.3) was custom made.

The link parts are machined by precision milling and wire cutting (WEDM) to minimize manufacturing error; for the secure fit of the link joints, accurate production of parts as close to the CAD modeling as possible is necessary. For the links, duraluminum (A7075) is used for its relatively light weight and strength. A total of 21 mini ball bearings are used to ensure smooth operation while the simulator is in motion.

For the prototype, a CCD color camera with a resolution of 250000 pixels and is 22 mm x 22 mm x 22 mm in volume is fixated at the base. While in motion, the links that are adjoined to this base are kept from protruding forward, while maintaining a constant center of rotation. The links keep their range of motion tight in their sides as well; therefore, it is possible to put another simulator right next to it. The simulator is 72.5 mm wide, and two of these devices can be appropriately installed in a robot head.

3. INVERSE KINEMATICS OF THE LINK ARCHITECTURE

The inverse kinematics of the oculomotor simulator's link architecture can be solved using multiple rotation matrices between the joint connections. Here, the Product of Exponential (POE) parameters [13] are used to calculate the behavior of the end-effector. Further details on the kinematics of this type of manipulators can be found in the papers on the agile eye [10].

Using POE parameters, the kinematics of chain or multilink mechanisms can be represented in the product of the joint twists. The rotation around the joint axis ω with a rotational angle θ is given by matrix R in (1).

$$R = e^{\hat{\omega}\theta} \tag{1}$$

From its definition, $\hat{\omega}$ is a skew-symmetric matrix where ω_1, ω_2, and ω_3 are the components of axis vector ω.

$$\hat{\omega} = \begin{bmatrix} 0 & -\omega_3 & \omega_2 \\ \omega_3 & 0 & -\omega_1 \\ -\omega_2 & \omega_1 & 0 \end{bmatrix} \tag{2}$$

Defining $v_\theta = 1 - \cos\theta$, $c_\theta = \cos\theta$, and $s_\theta = \sin\theta$, (1) can be written as (3).

$$R = e^{\hat{\omega}\theta} = I + \hat{\omega}\sin\theta + \hat{\omega}^2(1-\cos\theta) = \begin{bmatrix} \omega_1^2 v_\theta + c_\theta & \omega_1\omega_2 v_\theta - \omega_3 s_\theta & \omega_1\omega_3 v_\theta + \omega_2 s_\theta \\ \omega_1\omega_2 v_\theta + \omega_3 s_\theta & \omega_2^2 v_\theta + c_\theta & \omega_2\omega_3 v_\theta - \omega_1 s_\theta \\ \omega_1\omega_3 v_\theta - \omega_2 s_\theta & \omega_2\omega_3 v_\theta + \omega_1 s_\theta & \omega_3^2 v_\theta + c_\theta \end{bmatrix} \tag{3}$$

In the case of the oculomotor simulator, there are multiple links and joints which can be parameterized in a similar way; since there are three joints in a set, as shown in Fig. 4(a), three sets of rotational angles and rotational axis variables determine the rotational matrices. Fig. 4(a) and 4(b) are the schematic drawings of link set 1 (subscripts represent the link set and there are three sets in this simulator), which controls one axis of the eyeball position. Fig. 4(c) illustrates the consecutive movement of one set of links when the outer link is rotated arbitrarily. These joints of the link include; u_1 that connects the motor

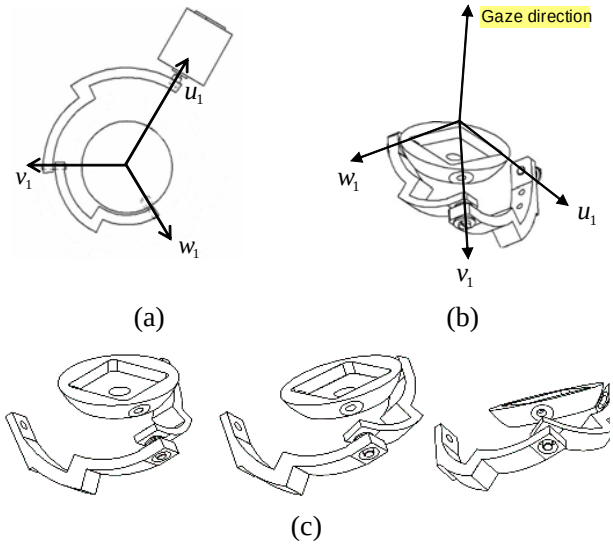

(a) Link set 1 with three rotational joints.
(b) Three joints and corresponding gaze direction.
(c) Consecutive movements in the links when the outer link is rotated.

Fig. 4. Link joint relationships.

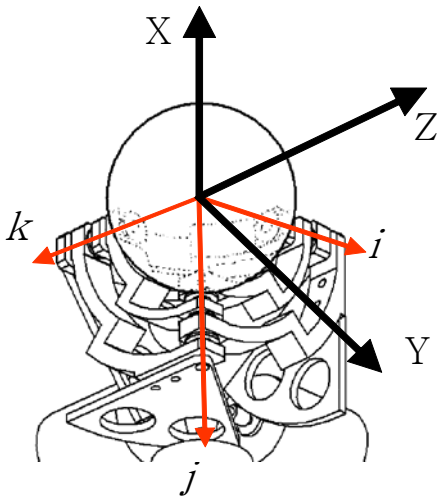

Fig. 5. The gaze direction coordinate frame in X, Y, and Z axes and the link frame in i, j, and k axes.

shaft to the outer link; v_1 that connects the outer link to the inner link; and w_1 that connects the inner link to the camera frame. For a simulator with three identical sets of parallel links that are stacked on top of each other, the form of rotation matrices is identical.

Since the outer link rotates along joint u_1, joint v_2's direction is found using (4) where v_{1o} is the initial direction vector of joint position v_1 and θ is the rotational angle of joint u_1. Likewise, w_1 is obtained by knowing the initial direction vector position of w_{1o}, and the rotational angle about v_1. The same process can be carried out for link set 2 and 3.

$$v_1 = e^{\hat{u}_1\theta} v_{1o} \tag{4}$$

To orient the simulator's camera in the desired direction, each actuator's angle of rotation (θ) in link axis is needed. (5) displays the initial direction vectors of each joint where {i, j, k} values are as given in (6) and the coordinate frames are as shown in Fig. 5.

$$\begin{bmatrix} u_{1o} \\ v_{1o} \\ w_{1o} \end{bmatrix} = \begin{bmatrix} i \\ j \\ k \end{bmatrix}, \begin{bmatrix} u_{2o} \\ v_{2o} \\ w_{2o} \end{bmatrix} = \begin{bmatrix} j \\ k \\ i \end{bmatrix}, \begin{bmatrix} u_{3o} \\ v_{3o} \\ w_{3o} \end{bmatrix} = \begin{bmatrix} k \\ i \\ j \end{bmatrix} \tag{5}$$

$$\begin{bmatrix} i \\ j \\ k \end{bmatrix} = \begin{bmatrix} -\frac{1}{\sqrt{3}} & 0 & \frac{\sqrt{2}}{\sqrt{3}} \\ -\frac{1}{\sqrt{3}} & \frac{\sqrt{2}}{2} & -\frac{1}{\sqrt{6}} \\ -\frac{1}{\sqrt{3}} & -\frac{\sqrt{2}}{2} & -\frac{1}{\sqrt{6}} \end{bmatrix} \tag{6}$$

With the initial boundary conditions, the position of v_1 is found in (7) by using the POE parameters for the joint. The rotation matrix in the form of (3) is substituted into (4) to produce (7) while θ is obtained by knowing the orthogonal nature of the links: w_1 and v_1 axes are always perpendicular to each other. Since, $w_1 \cdot v_1 = 0$, (7) leads to (8).

$$\begin{aligned} v_1 &= e^{\hat{u}_1\theta} v_{1o} \\ &= \begin{bmatrix} \left(-\frac{1}{\sqrt{3}}\right)^2 v_\theta + c_\theta & -\frac{\sqrt{2}}{\sqrt{3}} s_\theta & -\frac{1}{\sqrt{3}}\frac{\sqrt{2}}{\sqrt{3}} v_\theta \\ \frac{\sqrt{2}}{\sqrt{3}} s_\theta & c_\theta & -\frac{1}{\sqrt{3}} s_\theta \\ -\frac{1}{\sqrt{3}} \omega_3 v_\theta & -\frac{1}{\sqrt{3}} s_\theta & \left(\frac{\sqrt{2}}{\sqrt{3}}\right)^2 v_\theta + c_\theta \end{bmatrix} \begin{bmatrix} -\frac{1}{\sqrt{3}} \\ \frac{\sqrt{2}}{2} \\ -\frac{1}{\sqrt{6}} \end{bmatrix} \\ &= \begin{bmatrix} -\frac{\sqrt{3}}{3}(\cos\theta + \sin\theta) \\ \frac{\sqrt{2}}{2}(\cos\theta - \sin\theta) \\ -\frac{\sqrt{6}}{6}(\cos\theta + \sin\theta) \end{bmatrix}, \end{aligned} \tag{7}$$

$$\begin{aligned} &w_{11}\left(-\frac{\sqrt{3}}{3}(\cos\theta + \sin\theta)\right) + w_{12}\left(\frac{\sqrt{2}}{2}(\cos\theta - \sin\theta)\right) \\ &\quad + w_{13}\left(-\frac{\sqrt{6}}{6}(\cos\theta + \sin\theta)\right) = 0. \end{aligned} \tag{8}$$

Then the trigonometry identity, $\sin^2\theta_i + \cos^2\theta_i = 1$, and (8) can be simultaneously solved to find four θs for one axis; θ value, which satisfies the geometric conditions of the simulator, is chosen. Naturally, the rest of the motor angles in *i*, *j*, and *k* axis frame are solved using the same procedures to operate in the desired gaze direction's X, Y, and Z coordinate frame. In the gaze direction coordinate frame, which is shown in Fig. 5, X, Y, and Z are the torsional axis, the horizontal (left-right eyeball movement) axis, and the vertical (up-down eyeball movement) axis respectively.

4. WORKING RANGE OF THE OCULOMOTOR SIMULATOR

The unique spherical link shape having a bent in midarc allows strategic placement of inner and outer layer of links while all the links stay behind the camera. However, the range of motion is somewhat limited due to this design architecture; although the links do not protrude toward the camera plane while in motion, the links may collide as they close in toward the center. Extracting the collision locations require much cumbersome calculation. Here, for the purpose of defining the maximum range of motion, the collision was located using a computer simulation.

In the case of the human eyeballs that rotate with 3-DOF motion, the torsional eye position is not arbitrarily but uniquely determined by the gaze direction. Listing's law defines the ocular torsion in (9), and approximates it to be (10). Reference 14 finds the error in (10) to be within 0.5 degrees. The angles in (9) and (10) represent the rotational angles in Fick gimbal [14]. In a Fick gimbal, the eye positions are completely characterized first by the rotation around the vertical axis e_1 by θ_F, followed by rotation around the horizontal axis e_2 by ϕ_F and then by rotation around the torsional axis e_3 by φ_F.

$$r = r(e_3,\theta_F) \circ r(e_2,\theta_F) \circ r(e_1,\theta_F)$$
$$= \frac{1}{1+\tan(\theta_F/2)*\tan(\phi_F/2)*\tan(\varphi_F/2)} * \begin{pmatrix} \tan(\varphi_F/2) - \tan(\theta_F/2)*\tan(\phi_F/2) \\ \tan(\phi_F/2) + \tan(\theta_F/2)*\tan(\varphi_F/2) \\ \tan(\theta_F/2) - \tan(\phi_F/2)*\tan(\varphi_F/2) \end{pmatrix} \quad (9)$$

$$\varphi_F \approx \frac{\theta_F \cdot \phi_F}{100} \quad (10)$$

To define the range of motion of the simulator, two cases have been studied: with (3-DOF) and without (2-DOF) torsion. For this, the simulator was reconstructed in software and was rotated about three axis of the eye (camera) coordinate frame. For the 2-DOF case of the simulator, the collision-free area was found after rotating the simulator around Y and Z axis (see Fig. 5) while having the X axis, the torsion axis, restrained. The corresponding angles are plotted in Fig 6. Fig 6 is plotted for every 5 degrees Y and Z axes rotated in their polar coordinate until a collision occurs. In this figure, the dashed line shows the range of motion when the simulator's torsional movement is restrained - as if it were a 2-DOF device. In the same figure, the area enclosed by the solid line shows the case when the torsion movement is enabled. Here, the most conservative operating range of the simulator is found to be ± 33 degrees.

Studying the results of the simulation, the range of motion is maximized according to the optimized position of the arc bents along the links. This optimization process was not carried further in this paper. In order to increase the operating range of the simulator, the simulator is tested with a bias torsion in the initial position. In Fig. 7, the oculomotor simulator is given an initial torsion of 15 degrees and the range of the motion is increased to ± 42 degrees. These angular values still need to be optimized further to achieve the maximum operating range. With an optimized arc placements and an optimized bias torsion angle, the range of motion has the potential to increase significantly. Currently tested values of ± 42 or even ± 33 degrees are sufficient for the purpose of human oculomotor simulation: human eyes move within the range of ± 20 degrees about 90% of time [2].

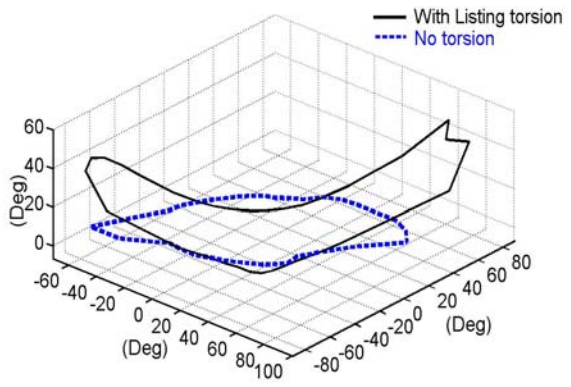

(a) Range of motion in 3D graph.

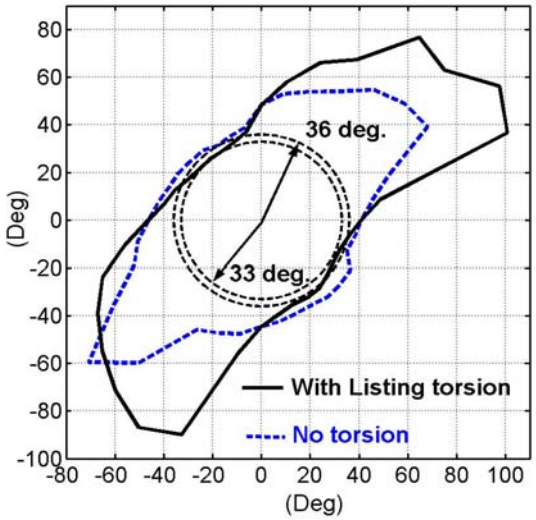

(b) Range of motion in 2D graph.

Fig. 6. The range of motion of simulator.

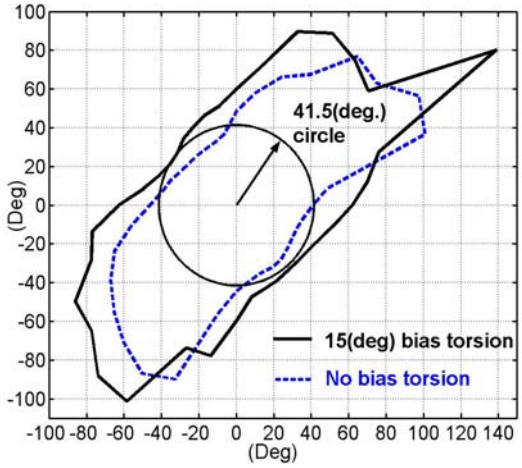

Fig. 7. Range of motion with a bias torsion.

5. PROTOTYPE PERFORMANCE EXPERIMENTS

The prototype of the 3-DOF Anthropomorphic Oculomotor Simulator requires its own control circuit to drive the actuators. Fig. 8 shows the control system of the oculomotor simulator. The actuator control circuit was built with LM629 motor control IC that receives encoder feedback data and produces PWM signals. The produced signals are fed into the H-bridge circuit amplifier (LM18200) and these amplified signals drive three actuators. To determine the static positional accuracy of simulator performance, the images captured by the camera are tested. For this, the oculomotor simulator is rotated around the horizontal, vertical and torsional axes. In order to measure the actual angular displacements, grid screens for each rotational axis are put in the front. The images in Fig. 9 are captured by camera when the prototype is rotated 30 degrees from the origin in each axis of rotation. These images are taken with the desired angle commands, which are sent to the control system. The visual readings prove to be quite accurate as seen in Fig. 10.

To see if the simulator can mimic the human eye accurately and realistically, actual human eye movements and the simulator movements are compared. Actual human eye movements are defined by gaze direction and its position signals are fed into the simulator to reproduce the same motion. The

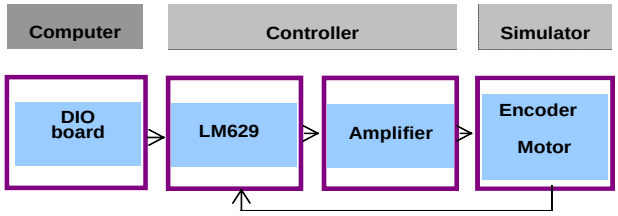

Fig. 8. Control system of the oculomotor simulator.

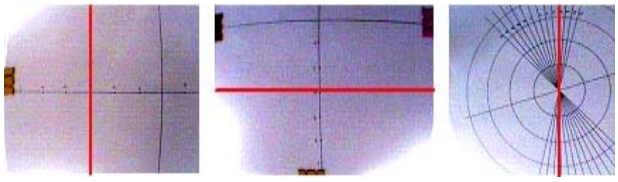

(a) (b) (c)

(a) Horizontal-camera rotation of 15 degrees to the right.
(b) Vertical-camera rotation of 15 degrees to the bottom.
(c) Torsional-camera rotation of 15 degrees in counter-clockwise rotation.

Fig. 9. The oculomotor simulator's actual angular displacements captured by camera.

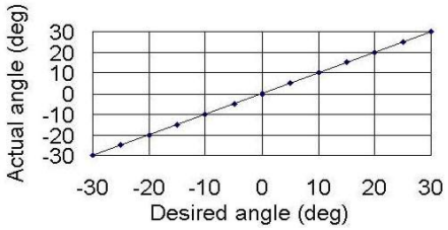

(a) Rotation about horizontal axis.

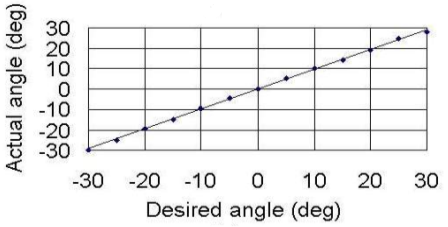

(b) Rotation about vertical axis.

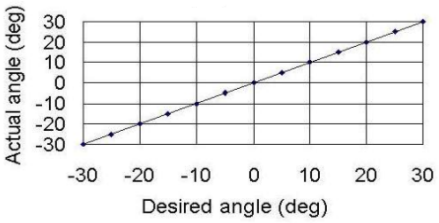

(c) Rotation about torsional axis.

Fig. 10. Comparison of actual and desired angles of the oculomotor simulator.

Fig. 11. The path of human eye's gaze on a web article.

prototype's dynamic performance test is performed by comparing movement of the human eye and the simulator when tracking a news article on a website. Fig. 11 displays the real human eyeball motion track in a bold line on a website [15]. The actual gaze path was collected using a scleral coil contact lens and electromagnetic recording process. For this process, a volunteer wore a scleral search coil contact lens [17] and entered an alternating magnetic field booth as shown in Fig 12.

This directional magnetic field booth is surrounded and wound with coils to produce two perpendicular

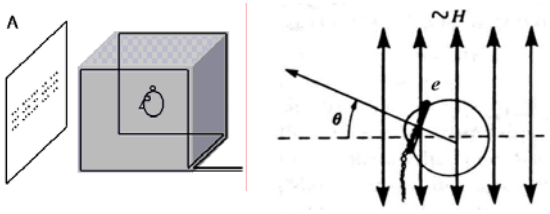

(a) (b)

(a) Magnetic field booth.
(b) The angular relationship between the eye and the magnetic field.

Fig. 12 . Eye movement measurement experiment.

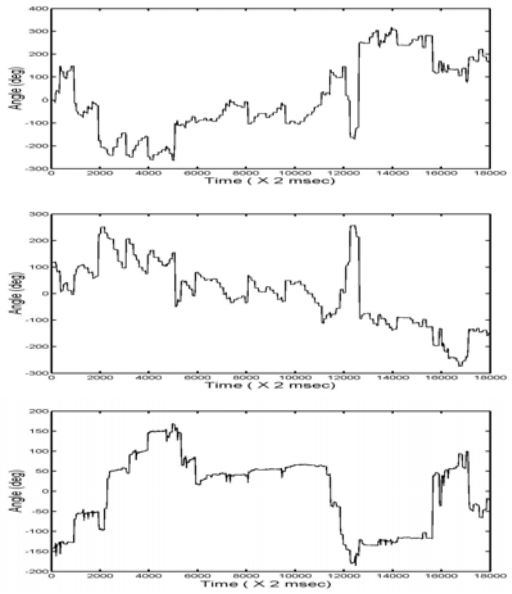

Fig. 13. Required rotational angles in actuators in each joint axis for tracking the eye movement on a website.

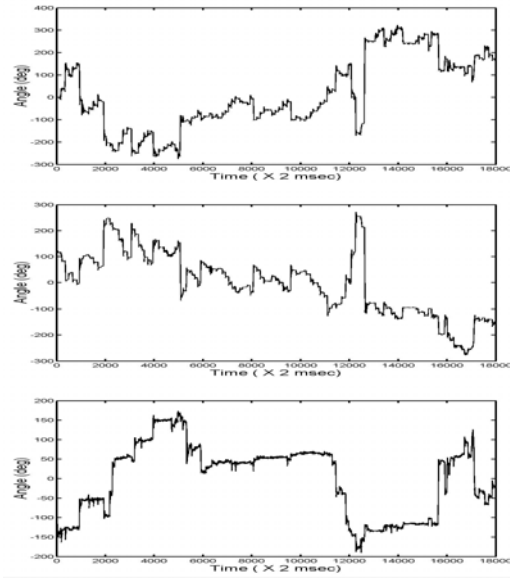

Fig. 14. Actual rotational angles in actuators in three actuator axes for tracking the eye movement on a website.

uniform magnetic fields inside the frame. Only one direction of the magnetic field generation set up is shown in Fig. 12(a). Each direction of the magnetic field is created with two sources of alternating currents with different frequencies. Because the contact lens is wound with coils to detect horizontal and vertical movement, the field induces an alternating voltage in the eye coil as the eye rotates. This voltage is proportional to the sine value of the angle between the lens coil and the direction of the magnetic field as seen in Fig. 12(b). The induced voltage signals are received by the electrodes on the lens and the actual gaze direction is determined by these signals [2,16,17]. Therefore, examining this change in voltage enables the magnetic mapping of the gaze path shown in Fig. 11 while the volunteer skims through an article on the web. The path data is collected every 2 ms.

The graphs of Fig. 13 display the calculated angular displacements in each joint axis of the simulator's frame (attached to the actuators). They are plotted with the values derived from the acquired x-y coordinate of the gaze direction, and the third torsional angle. The graphs of Fig. 14 exhibit the actuator's rotation measured by the encoder. Both sets of graphs match quite accurately, with no large overshoot (previous gimbals model potentially produced overshoot due to the high inertia of moving parts). This comparison confirms that the oculomotor simulator can sufficiently imitate human eye movement with a given gaze path.

6. CONCLUSIONS

Building and designing anthropomorphic humanoids has proven to be one of the most fascinating and challenging subjects in the robotics field. However, creating a human vision system has often been limited to simple versions of the image acquisition process inferior to the human eye's 3-DOF capabilities.

The unique link shape and the link orientation of the 3-DOF anthropomorphic oculomotor simulator architecture provide an unobstructed viewing range of the robotic eye. It fits within the given frame of a tight space such as a mask. Although, from this architecture, link collisions are inevitable limiting the range of motion, the achieved range of motion is sufficient for simulating most human eye movements. The simulator's oculomotor range is found to be ±33 degrees using a computer simulation. Also, further improvement in the working range is possible with a bias torsion at the initial position, and an optimized link bent placement.

Static tests on the prototype have shown favorable results, as the actual rotations in each axis match commands quite accurately. In testing the dynamic

performance of the simulator, the prototype is given data from an actual human eye movement. With the eye data collected while reading a website article, the simulator produced a gaze close to the given path of the real human eye.

The 3-DOF anthropomorphic oculomotor simulator presented in this paper demonstrates its applicability in life-sized humanoids. It successfully captures images and reproduces realistic human eye movements.

REFERENCES

[1] C. Breazeal, "Socially intelligent robots: Research, development, and applications," *Proc. of the IEEE Int Conf. on Systems, Man, and Cybernetics*, Tucson, Arizona, pp. 2121-2126, October 7-10, 2001.

[2] R. H. S. Carpenter, *Movements of the Eyes*, Pion Lt, 1998.

[3] M. Jenkin, E. Milios, J. Tsotsos, and B. Down, "A binocular robotic head system with torsional eye movements," *Int. J of Pattern Recognition and AI*, vol. 7, no. 1, pp. 51-68, 1993.

[4] C. Ishibiki, "Development of eye-ball robot as a bodily media and its applicability as a communication means," *Proc. of the 2001 IEEE/RSJ Int. Conf. on Intelligent Robots and Systems* Maui, Hawaii, pp. 1177-1182, Oct. 29-Nov. 3, 2001.

[5] A. Takanishi, T Matsuno, and I. Kato, "Developmemt of anthropomorphic head-eye robot with two eyes-coordinated head-eye motion and pursuing motion in the depth direction," *Proc. IROS*, pp. 799-804, 1997.

[6] N. Ferrier and J. Clark, "The Harvard binocular head," *Int. J. of Pattern Recognition and Artificial Intelligence*, pp. 9-31, Mar. 1993.

[7] K. Pahlavan and J. Eklundh, "Heads, eyes and head-eye systems," *Int. J. of Pattern Recognition and Artificial Intelligence*, vol. 7, pp. 33-49, Feb. 1993.

[8] C. Breazeal, A. Edsinger, P. Fitzpatrick, and B. Scassellati, "Active vision systems for sociable robots," in K. Dautenhahn (ed.), *IEEE Trans. on Systems, Man, and Cybernetics*, Part A, vol. 31, no. 5, pp. 443-453, 2001.

[9] C. M. Gosselin and J-F. Hamel, "The agile eye: A high performance three-degree-of-freedom camera-orienting device," *Proc. IEEE Int. Conf. on Robotics and Automation*, pp. 781-786, vol. 1, May 1994.

[10] C. M. Gosselin and E. Lavoie, "On the kinematic design of spherical three-degree-of-freedom parallel manipulators," *Int. J of Robotics Research*, vol. 12, pp. 394-402, 1993.

[11] Y. B. Bang, B. H. Shin, Jamie K. Paik, and C. Lee, "A Biomorphic Simulator of Three-Dimensional Eye Movements," *Proc. of IEEE Int. Conf. on Advanced Robotics*, Portugal, Jun 30-July 3, 2003.

[12] Y. B. Bang, Jamie K. Paik, B. H. Shin, and C. Lee, "The anthropomorphic oculomotor with the three-degree-of-freedom parallel link," *Proc. (CD) 35th Int. Symp. on Robotics*, Paris, 23-26 March, 2004.

[13] J. Craig, *Introduction to Robotics Mechanics and Control*, Addison Wesley, 1989.

[14] T. Haslwanter, "Mathematics of three-dimensional eye rotations," *Vision Research*, vol. 35, pp. 1727-1739, 1994.

[15] C. Lee, *Movements of the Gaze During Hangul Reading*, *Seoul National University Press*, 2004.

[16] C. Lee, "Eye and head coordination in reading: Roles of head movement and cognitive control," *Vision Research*, vol. 39, no. 22 pp. 3761-3768, 1999.

[17] D. A. Robinson, "A method of measuring eye movement using a scleral search coil in a magnetic field," *IEEE Trans. on Biomedical Eng*, vol. 10, pp.137-145, 1963.

Young-Bong Bang received the B.S. and M.S. in Mechanical Engineering from Seoul National University in 1989 and 1991. He received the Ph.D. in Precision Machine Engineering from The University of Tokyo in 1997. Professor Bang has been with Seoul National University since 2000.

Jamie K Paik received the B.A.Sc. with CAA option in Mechanical Engineering from University of British Columbia in 2002. Currently she is working toward her Ph.D. in Mechanical Engineering in Seoul National University. Her research interests include actuators and sports robots.

Bu-Hyun Shin received the B.S. in Mechanical Engineering from Seoul National University in 2001. He is working toward his Ph.D. in the same university. His research interests include mechatronics and humanoids.

Choongkil Lee received the B.A. in Psychology from Seoul National University in 1977. He received the Ph.D. from University of Illinois in 1986. Professor Lee has been with the Department of Psychology of Seoul National University since 1998. His research interests include physiology and psychology of vision.